High-frequency EPR on high-spin transitions-metal sites

Mathies, G.

Chapter 4

A W-band pulsed EPR/ENDOR study of Co(II)S_4 coordination in the Co[$(SPPh_2)(SP^iPr_2)N]_2$ complex

Spin-echo detection at 95 GHz enables an electron-paramagnetic-resonance study of a cobalt complex with a bio-mimetic coordination of the transition metal by four sulfur atoms. A magnetically diluted single crystal of the complex has been investigated in great detail. Electron-nuclear double-resonance signals were observed of ligand nuclei and complete hyperfine tensors of the distinct phosphorus nuclei were derived, assigned and discussed.

Silvia Sottini, Guinevere Mathies, Peter Gast, Dimitrios Maganas, Panayotis Kyritsis and Edgar J. J. Groenen, *Phys. Chem. Chem. Phys.*, 11 (2009) 6727-6732.

4.1 Introduction

Transition-metal ions with a sulfur-rich coordination sphere are abundant active sites in proteins and enzymes. [99] Bonding between metal ions and sulfur-containing ligands shows up in various coordination geometries and a correspondingly large flexibility exists with respect to electronic structure. [100] Among the biologically important redox-active transition-metal ions, manganese, iron and copper are most easily accessible and therefore usually constitute the catalytically active sites of redox metalloenzymes. [99] However, cobalt-based active sites have also been found in a number of enzymes. [101, 102] In addition to these native sites, cobalt sites have been created by substitution of Co^{2+} for Fe^{2+} or Cu^{2+}, [96, 103] and mostly for spectroscopically silent and diamagnetic metal ions like Zn^{2+} or Cd^{2+}. [104, 105] In the latter case, the reason for the substitution is that Co^{2+} sites are amenable to biophysical characterization by optical spectroscopy, magnetic susceptibility and magnetic resonance methods. In this context, cobalt analogue complexes have been synthesized to mimic the active sites in proteins and enzymes. [106] Here we consider such a complex in which cobalt is coordinated by four sulfurs.

The paramagnetic nature of the Co^{2+} $3d^7$ configuration enables the application of electron paramagnetic resonance (EPR) in the study of the electronic structure of the metal site. However, the high spin ($S = 3/2$) configuration in the typically encountered Co^{2+} sites complicates the use and interpretation of EPR because of the rather large zero-field splitting (ZFS) between the $\pm 1/2$ and $\pm 3/2$ Kramers doublets. Studies on Co(II)S_4 coordination by continuous-wave EPR at X band have been reported by Fukui *et al.* [75–77] In recent years, developments have taken place in EPR technology, which have largely enhanced the possibilities to investigate such paramagnetic centers. [107] In particular, this includes the development of spectrometers working at high magnetic fields and high microwave frequencies, i.e., much higher than the commonly used 9 GHz.

Recently we have studied two complexes with Co(II)S_4 coordination by EPR spectroscopy, namely $Co[(SPPh_2)_2N]_2$ and $Co[(SPPh_2)(SP^iPr_2)N]_2$, which will be denoted as $Co^{Ph,Ph}L_2$ and $Co^{iPr,Ph}L_2$, respectively. [5] Powders and single crystals of these compounds have been investigated by continuous-wave EPR spectroscopy at 9, 95 and 275 GHz. The ZFS, close to axial for $Co^{Ph,Ph}L_2$ and rhombic for $Co^{iPr,Ph}L_2$, has a magnitude of 23.8 and 29.6 cm^{-1}, respectively. For the corresponding diamagnetically diluted samples, 1% CoL_2 in the analogous ZnL_2 complex, the cobalt-hyperfine splitting was resolved and could be analyzed. Interpretation of the data in terms of the electronic structure, and in particular the characteristics of the cobalt-sulfur bonds, requires a study of the spin delocalization over the ligands. The present paper represents a first step in that direction.

In this work, we report on the $Co^{iPr,Ph}L_2$ complex [108] (Figure 4.1), which we investigated by pulsed EPR spectroscopy at 95 GHz (W band). Electron spin echoes (ESEs) have been detected for diamagnetically diluted $Co^{iPr,Ph}L_2/Zn^{iPr,Ph}L_2$

single crystals. Stimulated echoes were observed and pulsed electron-nuclear double-resonance (ENDOR) experiments were performed. The spectra show ENDOR signals from the ligand phosphorus, nitrogen and hydrogen atoms. The complete hyperfine tensors for the phosphorus atoms are derived, assigned and discussed.

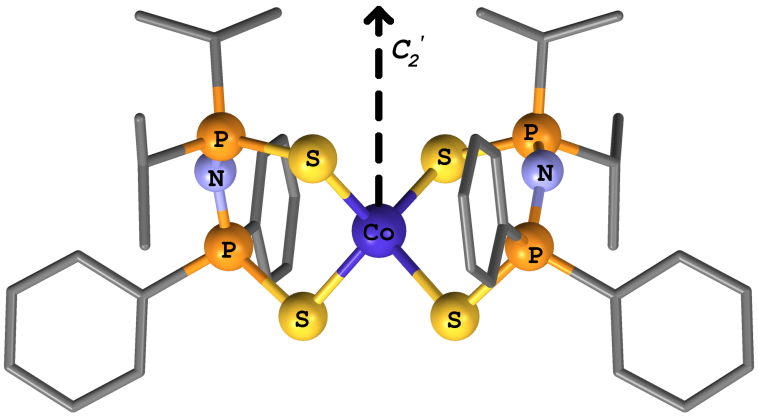

Figure 4.1: The molecular structure of $Co[(SPPh_2)(SP^iPr_2)N]_2$.

4.2 Materials and methods

Magnetically diluted single crystals of 1% $Co^{iPr,Ph}L_2$ in $Zn^{iPr,Ph}L_2$ have been investigated. A typical size of these co-crystals was $0.3 \times 0.5 \times 0.7$ mm, and the synthesis of the complex is described in reference 108. The crystal was mounted in a quartz tube of inner diameter 0.60 mm and outer diameter 0.84 mm, which was placed into the cylindrical cavity of our homebuilt W-band spectrometer, [82] which was upgraded recently. The sample tube and the magnet can be rotated around independent axes thus enabling experiments at every possible orientation of the magnetic field with respect to the crystal, without remounting the crystal. The sample was kept for one week under helium atmosphere before measuring, because otherwise a background signal was present in the EPR spectra.

All the experiments were carried out at 1.6 K and at a microwave frequency of 94.9 GHz. For the EPR experiments, a two-pulse Hahn-echo sequence was employed using microwave pulses of 80 and 160 ns separated by 140 ns at a repetition rate of 10 kHz. For the ENDOR experiments, a Mims type three-pulse sequence was used. The three microwave pulses had a length of 100 ns. The time between the first and the second microwave pulse was 220 ns, the time between the second and the third microwave pulse had a variable length. The length of the radio-wave pulse varied with the orientation between 20 and 60 ms, because the relaxation times change with

the orientation of the magnetic field with respect to the crystal. The repetition rate was 1 kHz. Data analysis was performed using a Matlab version of the optimization package Minuit (CERN).

4.3 Theoretical background

The description of the EPR and ENDOR spectra of the high-spin Co^{2+} complex ($S = 3/2$) starts from an electron spin Hamiltonian, which includes the zero-field splitting (ZFS) and the electron Zeeman interaction

$$H_e = \vec{S} \cdot \vec{\vec{D}} \cdot \vec{S} + \mu_B \vec{B} \cdot \vec{\vec{g}} \cdot \vec{S} \tag{4.1}$$

where $\vec{S}$ represents the electron-spin angular momentum operator and the D and g tensors represent the interactions. A full description of the $S = 3/2$ case can be found in textbooks. [109]

The ZFS gives rise to two Kramers doublets and, although m_s is not a good quantum number, we will refer to these as $\pm 1/2$ and $\pm 3/2$. In a small magnetic field, such that the electron Zeeman interaction is much smaller than the zero-field interaction, the energy of the four levels may be obtained by considering the doublets separately. In this effective spin 1/2 picture, the energies for both the $\pm 1/2$ and $\pm 3/2$ doublet may be written as

$$E = \pm \frac{1}{2} \mu_B B \sqrt{\sum_\beta \left(\sum_\alpha \ell_\alpha g'_{\alpha\beta} \right)^2} \tag{4.2}$$

Here $\alpha, \beta = x, y, z$ and $\vec{\ell}$ represents a unit vector in the direction of $\vec{B}$ in the reference axes system x, y, z. The effective g' matrix is defined by

$$g'_{\alpha\beta} = g_{\alpha\beta} \omega_\beta \tag{4.3}$$

with

$$\begin{aligned} \omega_x &= 2\sqrt{3} \cos\theta \sin\theta + 2 \sin^2\theta \\ \omega_y &= 2\sqrt{3} \cos\theta \sin\theta - 2 \sin^2\theta \\ \omega_z &= 3 \cos^2\theta - \sin^2\theta \end{aligned} \tag{4.4}$$

for the $\pm 3/2$ doublet. The corresponding expressions for the $\pm 1/2$ doublet are obtained by replacing $\cos\theta$ by $-\sin\theta$ and $\sin\theta$ by $\cos\theta$. The angle θ is related to the ZFS parameters by $tg2\theta = \sqrt{3}E/D$.

For $Co^{iPr,Ph}L_2$ the splitting between the doublets in zero field amounts to about 900 GHz as compared to the microwave quantum of 94.9 GHz. The EPR transition

in the low-temperature W-band spectrum corresponds to the transition within the Kramers doublet of lowest energy. From the cw EPR study on $Co^{iPr,Ph}L_2$ at X band, we found $E/D = -0.33$. [5] The ZFS is maximum rhombic, which implies that the difference in the expressions in Equation 4.4 for the $\pm 1/2$ and $\pm 3/2$ doublets corresponds to an interchange of the x and z labels. The ω values are the same. Consequently, whether the $\pm 1/2$ and $\pm 3/2$ doublet is the lowest, cannot be concluded. From here on, we will consider D to be negative, which corresponds to the assumption that $\pm 3/2$ is the lowest Kramers doublet. Our results are not dependent upon this choice, because of the rhombicity of the ZFS tensor.

The principal axes of the g' tensor at W band are parallel to those of the ZFS tensor owing to the negligible contribution of the off-diagonal terms of the g tensor to the g' tensor. This allows us to translate the experimental data into the reference system in which the ZFS tensor is diagonal.

In order to describe the phosphorus ($I = 1/2$) ENDOR spectra, we have to consider the nuclear Zeeman interaction and the hyperfine interaction. In case the mixing of the electron-spin states by the hyperfine interaction is negligible, the nuclear spin Hamiltonian may be written as

$$H_n = -g_P \mu_n \vec{I} \cdot \vec{B} + \langle \vec{S} \rangle \cdot \vec{\vec{A}} \cdot \vec{I} \tag{4.5}$$

where $\langle \vec{S} \rangle$ represents the expectation value of the electron-spin angular momentum. This expectation value can be calculated from the electron-spin eigenstates obtained through the exact diagonalization of the electron spin Hamiltonian.

For each phosphorus nuclear spin interacting with the electron spin, two transitions may show up in the ENDOR spectrum, symmetrically shifted with respect to the phosphorus nuclear Zeeman frequency.

4.4 Results

ESE-detected EPR spectra of a single crystal of 1% $Co^{iPr,Ph}L_2/Zn^{iPr,Ph}L_2$ have been obtained for many orientations of the magnetic field with respect to the crystal. The measurements were carried out in the $x'y'$, $y'z'$ and $z'x'$ planes, where x',y',z' refers to the principal axes system of the effective g' tensor. In Figure 4.2, spectra for orientations of the field in the $y'z'$ and $x'y'$ planes are shown. For each orientation we observe a single line. For orientations close to z', the line reveals sub-structure owing to the resolved cobalt hyperfine interaction. The system shows a marked anisotropy in T_2, which affects the intensity of the resonant line for different orientations of the field, and in T_1. Both become faster on going towards z'. The effective g' tensor was extracted from the data using Equation 4.2 and its principal values at W band are 1.61, 2.34 and 6.42.

The ENDOR spectrum measured on the same crystal in the frequency range up to 150 MHz and for an orientation of the magnetic field along y' is shown in Figure 4.3.

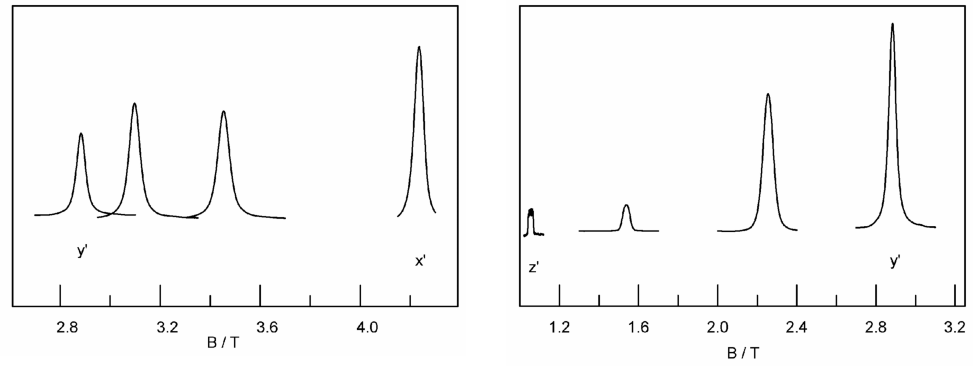

Figure 4.2: W-Band ESE-detected EPR spectra of a crystal of 1% $Co^{iPr,Ph}L_2/Zn^{iPr,Ph}L_2$ at different orientations of the magnetic field with respect to the crystal. The spectra in the upper figure correspond to orientations in the $x'y'$ plane, in the lower figure in the $z'y'$ plane. At z' the cobalt hyperfine splitting of the line is resolved.

Signals around the nuclear Zeeman frequency of nitrogen, phosphorus and hydrogen are easily recognizable. There is a fourth, broader signal in the spectrum, which might derive from cobalt.

Zooming into the phosphorus region of the spectrum, Figure 4.4 shows the ENDOR spectrum for an orientation of the magnetic field in the $x'y'$ plane. Four ENDOR transitions are seen between 58 and 62 MHz, one of which shows a line width different from the others. The ENDOR frequencies are not symmetrically displaced around the nuclear Zeeman frequency of phosphorus, i.e., 59.586 MHz for a magnetic field of 3.454 T. The ENDOR spectra were obtained for many other orientations of the magnetic field with respect to the crystal, adjusting the field strength to remain in resonance with the EPR transition. Orientations were chosen in five planes, three of which concerned the principal planes of the effective g' tensor. For none of the orientations more than four ENDOR lines were found in the phosphorus region. The repetition rate was varied between 1 kHz and 1 Hz in order to check for saturation of nuclear transitions, but no extra lines showed up. In addition, experiments were performed varying the length of the rf pulse during the mixing period, the power of the rf pulse and the duration of the mixing period. Also in these experiments no other lines were detected. For certain orientations of the field in the $x'y'$ plane, lines with deviating width and shape were observed. These were not taken into account for the subsequent analysis.

Resonances belonging to four distinct phosphorus nuclei can be followed through the planes. The A tensors were derived from the data using Equation 4.5, in which we assumed that the observed ENDOR lines correspond to the electron-spin β manifold.

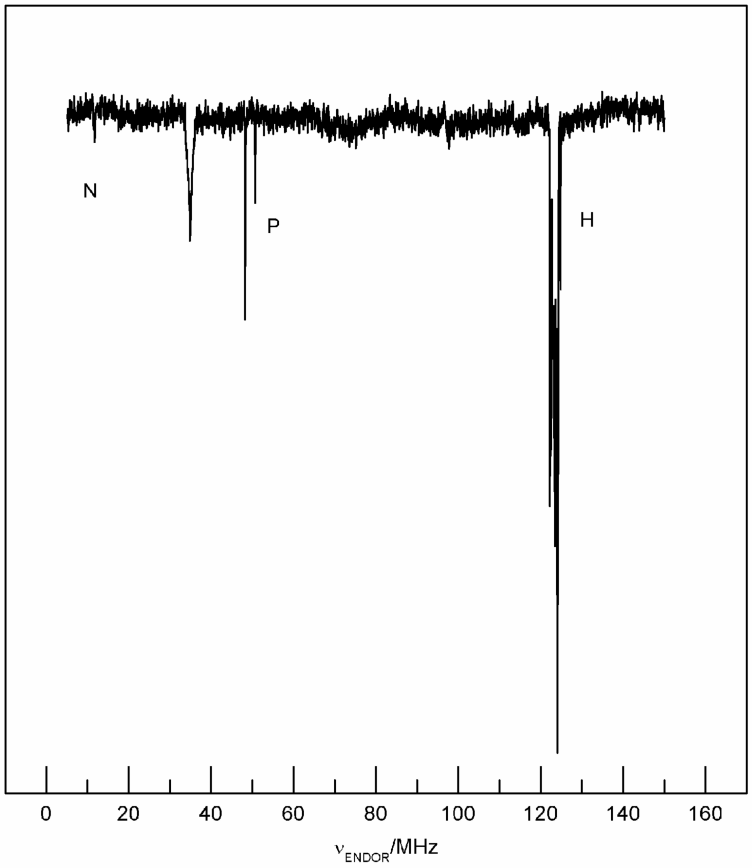

Figure 4.3: The pulsed ENDOR spectrum of a single crystal of 1% $Co^{iPr,Ph}L_2/Zn^{iPr,Ph}L_2$ with the magnetic field parallel to the y' axis of the g' tensor and $B = 2.884$ T. In the spectrum, resonances due to hydrogen, phosphorus and nitrogen nuclei are observed.

Under the assumption that the principal axes system of the g tensor coincides with that of the ZFS tensor, i.e., that the off-diagonal terms of the g tensor are negligible, the g values were derived from the ESE-detected EPR data using Equation 4.1 and the ZFS parameters D and E of -387 and 126 GHz, as known from the cw EPR study on $Co^{iPr,Ph}L_2$. [5] Subsequently, the electron spin Hamiltonian was diagonalized and the expectation value $\langle\vec{S}\rangle$ calculated. Finally, a fit of the observed ENDOR frequencies using Equation 4.5 was performed. Figure 4.5 shows the quality of the fits for all the planes investigated. Most of the frequencies not taken into account in the fit (the open dots in Figure 4.5) also are on the lines that result from the fit. Some of these frequencies in the $x'y'$ plane slightly deviate, but the deviations are within the line widths of the corresponding ENDOR lines.[1] The resulting four A

[1] After publication of this work it was realized that these deviations arise from what Abragam

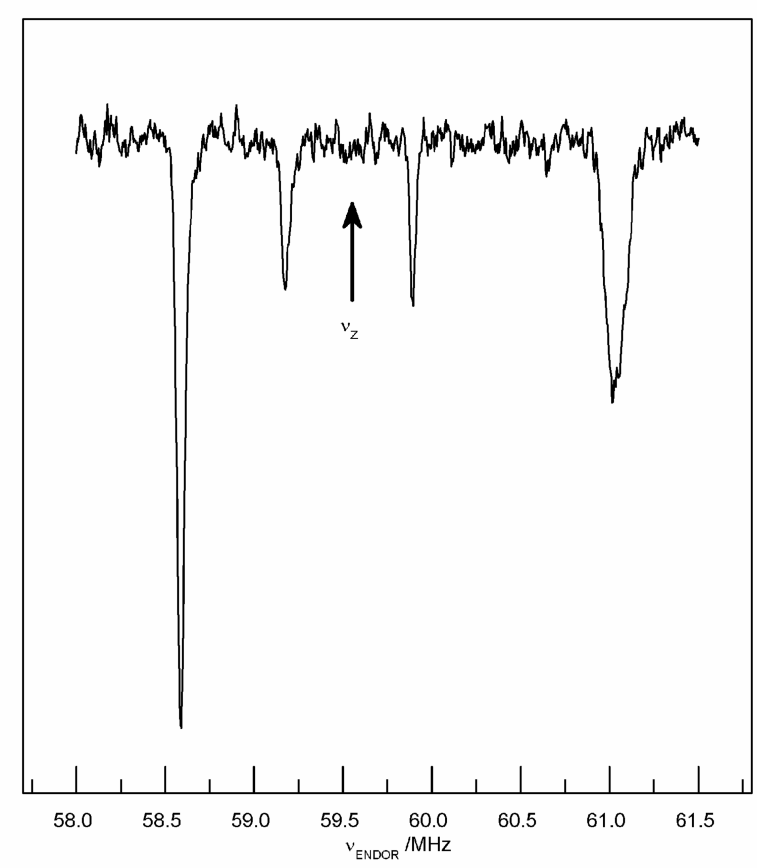

Figure 4.4: The pulsed ENDOR spectrum of a single crystal of 1% $Co^{iPr,Ph}L_2/Zn^{iPr,Ph}L_2$ taken at 40 degrees from x' in the $x'y'$ plane of the g' tensor at a field strength of 3.454 T. The spectrum shows four ENDOR lines in the region around the nuclear Zeeman frequency (ν_Z) of phosphorus.

tensors are presented in Table 4.1. The tensors A_1 and A_2 are similar, as well as the tensors A_3 and A_4.

The analysis relies on the assumption that the principal axes of the ZFS and g tensors coincide and on the values of D and E. In order to estimate the uncertainty in the A tensors that results from these assumptions, we varied the ratio E/D in the range $(-0.3, -0.333)$ and the values of D and E by 10%, while their ratio was kept the same. In all cases, variations in the elements of the A tensors were limited to 1 to 2%. We also considered off-diagonal terms in the g tensor of the order of 0.025, which led to variations between 1 and 7% in the elements of the A tensors.

and Bleaney call the pseudo-nuclear Zeeman effect. [3] Recently Sottini and Groenen [110] revisited the perturbation approach followed by Abragam and Bleaney and showed that the name pseudo-nuclear Zeeman effect does not do justice to its physical nature.

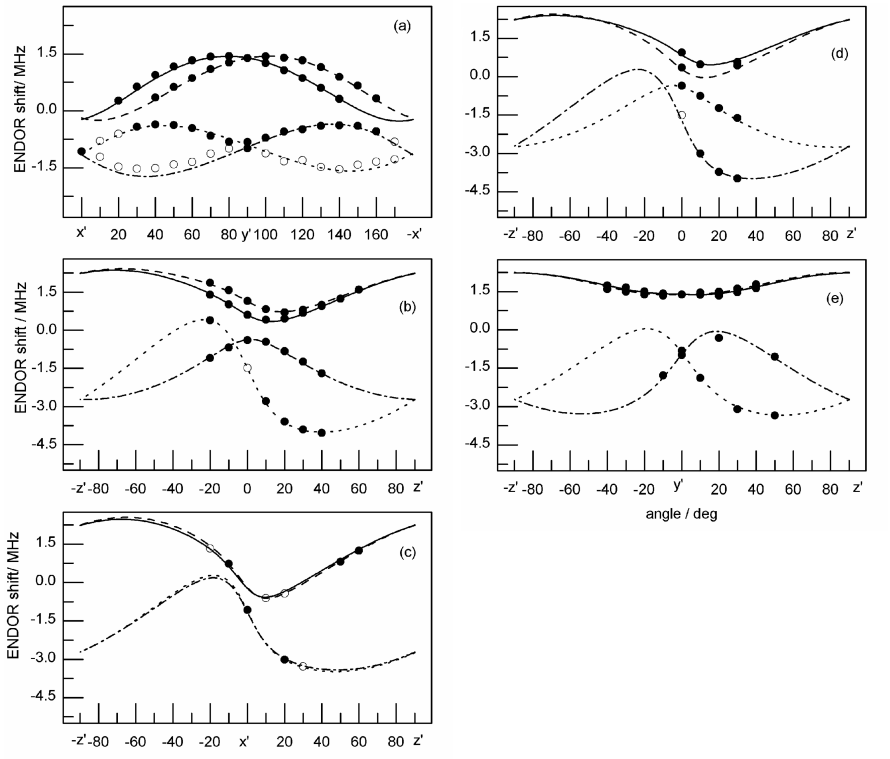

Figure 4.5: The phosphorus ENDOR resonances as a function of the orientation of the magnetic field in the following planes: $x'y'$ (a), -50 degrees from x' in the $x'y'$ plane towards z' (b), $z'x'$ (c), 40 degrees from x' in the $x'y'$ plane towards z' (d) and $z'y'$ (e). The dots represent the data points, the lines are the fits based on Equation 4.5. The ENDOR shift is defined as $\nu_Z - \nu_{ENDOR}$. The open dots represent the points with deviating width and shape that have been omitted in the fitting procedure.

In any case, the above analysis was found superior to the alternative approach of working in the effective spin 1/2 picture. In that case, no assumptions as regards the g tensor are necessary. At W band, the treatment of the Zeeman term as a first order perturbation with respect to the ZFS term in Equation 4.1 leads to energies that still provide an adequate description of the EPR spectra. However, for the interpretation of the ENDOR spectra we need the eigenstates and the effective spin 1/2 treatment was found to introduce appreciable errors in the expectation value $\langle\vec{S}\rangle$. Too low expectation values were found, with deviations up to 40% for some orientations. In spite of this, the directions of the principal axes of the A tensors came out the same in both treatments.

A_1/h			A_2/h		
0.38	−0.45	−0.71	0.30	0.51	−0.80
−0.45	−2.06	0.02	0.51	−2.05	−0.01
−0.71	0.02	−1.65	−0.80	−0.01	−1.66
A_3/h			A_4/h		
2.49	−1.00	−1.42	2.63	1.16	−1.35
−1.00	1.20	1.19	1.16	1.28	−1.11
−1.42	1.19	1.83	−1.35	−1.11	1.84

Table 4.1: Hyperfine tensors of the four phosphorus nuclei as obtained from the fit of the ENDOR frequencies using Equation 4.5. The hyperfine values are expressed in MHz. The tensors are represented in the reference frame of the g' tensor (x', y', z'). The sign of the tensor elements corresponds to the assumption that the ENDOR signals derive from the β manifold.

4.5 Discussion

The coordination of Co^{2+} to sulfur containing ligands in Co(II)S_4 chemical or biological sites is difficult to study by EPR because of the large ZFS of the $S = 3/2$ high-spin configuration. At W band, ESE-detected EPR and ENDOR experiments have been found feasible for a 1% $Co^{iPr,Ph}L_2/Zn^{iPr,Ph}L_2$ single crystal. The EPR and ENDOR spectra were studied as a function of the orientation of the magnetic field with respect to the crystal. In the ENDOR spectra, signals were identified from phosphorus, nitrogen and hydrogen atoms of the coordinated ligand and they present the possibility of a quantitative analysis of the delocalization of the electron-spin density beyond the Co(II)S_4 core. Interactions between a Co^{2+} site and distant phosphorus atoms have been investigated in the cobalt-substituted zinc finger 3 of transcription factor III A. [79]

In our system we have been able to fully analyze the phosphorus ENDOR data and the complete hyperfine tensors are given in Table 4.1. In order to discuss these results, we first describe the crystal structure of the $Co^{iPr,Ph}L_2$ complex.

The $Co^{iPr,Ph}L_2$ complex crystallizes in the C2/c space group with four magnetically indistinguishable molecules in the unit cell. [108] The CoS_4 core has D_{2d} symmetry, but the symmetry of the complex is lower because the two phosphorus atoms in each CoSPNPS ring (Figure 4.1) carry different peripheral groups (^{i}Pr and Ph). Only one two-fold rotation axis is left, which is indicated by C_2' as it is perpendicular to the S_4 axis of the core. The C_2' axis bisects the exo S−Co−S angles and is parallel to the crystallographic b axis. The complex adopts the so-called "bird-

arrangement". In view of the near equivalence observed for the structures of the analogous CoL_2 and ZnL_2 complexes, we assume that the description of the structure of the $Co^{iPr,Ph}L_2$ complex as derived from the crystal structure also applies to the structure of the complex in the mixed 1% $Co^{iPr,Ph}L_2/Zn^{iPr,Ph}L_2$ crystal.

Recently we have performed a continuous-wave EPR study of $Co^{iPr,Ph}L_2$ at 9, 95 and 275 GHz. [5] At X band, the continuous-wave EPR spectrum of a mixed crystal, similar to the crystal investigated here, shows fully resolved cobalt ($I = 7/2$) hyperfine structure. An orientation study of this hyperfine structure revealed the coincidence of the principal axes of the effective g' tensor and the effective cobalt hyperfine tensor, although this is only enforced by symmetry for one of the axes, the one parallel to the C_2' axis. The principal axes of the g' tensor follow those of the ZFS tensor because of the negligible contribution of the off-diagonal elements of the g tensor to the g' tensor. Owing to the symmetry of the complex, one of the principal axis of the g tensor must also be parallel to the C_2' axis, and only one of the off-diagonal terms (g_{xz}, as we will see below) might be non-zero. The principal values of the g' tensor at X band are 1.62, 2.38 and 6.44. [5]

The ESE-detected EPR spectra at W band are consistent with the interpretation of the continuous-wave spectra at X band. The four molecules in the unit cell are magnetically indistinguishable and, for each orientation of the magnetic field with respect to the crystal, a single line is observed. As expected, the principal values of the g' tensor, 1.61, 2.34 and 6.42, slightly differ from the ones obtained at X band. The description in terms of an effective $S = 1/2$ spin is less applicable at W band than at X band, because the intra-doublet splitting (the microwave quantum) is about 10% of the inter-doublet splitting. The limits of such a description at W band are found to concern much more the eigenstates than the eigenvalues. The cobalt hyperfine structure, resolved at X band for all orientations of the magnetic field, is largely anisotropic and biggest for the magnetic field parallel to z'. Only along this direction the cobalt hyperfine structure is resolved in the ESE detected EPR spectra at W band.

For the interaction of the electron spin and a phosphorus nuclear spin $I = 1/2$, the ENDOR spectrum is expected to consist of two lines symmetrically displaced with respect to the phosphorus nuclear Zeeman frequency. The $Co^{iPr,Ph}L_2$ complex contains four phosphorus nuclei and eight lines are expected. For none of the orientations of the magnetic field with respect to the crystal are more than four lines observed in the ENDOR spectrum, and no more than two on either side of the nuclear Zeeman frequency. Moreover, the ENDOR shift of the lines above and below the nuclear Zeeman frequency is not identical. We conclude that the lines derive from the four phosphorus nuclei and that for each nucleus only one ENDOR line shows up, either above or below the nuclear Zeeman frequency. A difference in the intensity of the ENDOR lines on either side of the nuclear Zeeman frequency has been observed before in experiments at large thermal polarization. [111, 112] It is related to relaxation in the spin system. The systematic absence of one of the

ENDOR lines in our case deserves further attention. The deviating width and shape of some of the ENDOR lines, like the one to the right in Figure 4.4, most probably results from a slight magnetic inequivalence of the four molecules in the unit cell, which shows up at the ENDOR level (100 kHz).

Each of the phosphorus hyperfine tensors A_1, A_2, A_3, A_4 in Table 4.1 corresponds to one of the phosphorus nuclei in the $Co^{iPr,Ph}L_2$ complex. The tensor elements of A_1 and A_2 have approximately equal magnitudes, while the $x'y'$ and $y'z'$ elements have opposite sign and the same holds for A_3 and A_4. We conclude that the A_1 and A_2 tensors belong to two phosphorus atoms that carry the same peripheral group (either ^{i}Pr or Ph) and are related by a two-fold rotation around y'. The principal y' axis of the g' tensor is consequently parallel to the C_2' axis of $Co^{iPr,Ph}L_2$. The same applies to A_3 and A_4. The fact that the magnitude of the tensor elements is similar, but not identical implies that the symmetry of the complex is only approximately C_2.

After diagonalization of the A tensors of the four phosphorus nuclei in Table 4.1, we arrive at the principal values, which carry an isotropic and an anisotropic part. The tensors A_1 and A_2 are similar, and the same holds for A_3 and A_4. In Table 4.2 we present the average diagonalized tensor for both types of phosphorus nuclei, one that belongs to the phosphorus that carry two Ph groups and one that belongs to the phosphorus that carry two ^{i}Pr groups.

	$A_{x''x''}/h$	$A_{y''y''}/h$	$A_{z''z''}/h$	A_{iso}/h
$P_{1,2}$	−1.07	−0.72	1.79	−1.13
$P_{3,4}$	−1.53	−0.99	2.52	1.88

Table 4.2: Hyperfine tensors of the two types of phosphorus nuclei. The principal values of the anisotropic hyperfine tensors and the isotropic hyperfine values are expressed in MHz. The principal axes systems of the hyperfine tensors are indicated by (x'', y'', z''). The sign of the tensor elements corresponds to the assumption that the ENDOR signals derive from the β manifold.

To which phosphorus do the hyperfine tensors belong? A significant part of the spin density will be on cobalt. For spin density one on cobalt, at a distance of 0.33 nm from phosphorus, the dipolar contribution to the anisotropic hyperfine tensor of the phosphorus would be −0.8 MHz, −0.8 MHz, 1.6 MHz. The ratio of these principal values amounts to −1, −1, 2. The correspondence of the signs of the dipolar contribution with the signs of the principal values of the anisotropic tensors in Table 4.2 corroborates our assumption that the observed ENDOR lines belong to the nuclear-spin transition in the electron-spin β manifold. Comparison with the tensors in Table 4.2 further shows that the principal values do not quantitatively

adhere to the dipolar ratio. This is not surprising because not only the spin density on cobalt contributes to the anisotropic part of the phosphorus hyperfine tensor. Nevertheless, if we calculate the angle between the direction of the principal z'' axes of the corresponding tensors A_1 and A_2, we find an angle of 161 degrees. From the crystal structure [108] we calculate an angle of 170 degrees between the vectors connecting the cobalt with the two phosphorus atoms that carry the Ph groups. The near equivalence of these angles leads to the conclusion that the tensors A_1 and A_2 most probably belong to the phosphorus atoms that carry the Ph groups ($P_{1,2}$ in Figure 4.1 and Table 4.2). Similarly, the principal z'' axes corresponding to the tensors A_3 and A_4 make an angle of 128 degrees, and the vectors connecting the cobalt with the two phosphorus atoms that carry the ^{i}Pr groups an angle of 119 degrees. [108] The tensors A_3 and A_4 most probably belong to the phosphorus atoms that carry the ^{i}Pr groups ($P_{3,4}$ in Figure 4.1 and Table 4.2). It should be noted that ^{31}P NMR studies of $Co^{iPr,Ph}L_2$ also made it possible to distinguish the two different types of phosphorus atoms. [108]

Finally a remark about the isotropic part of the phosphorus hyperfine tensors. The isotropic hyperfine interaction has different sign for the two types of phosphorus, negative for $P_{1,2}$ and positive for $P_{3,4}$. The small s-spin density is negative on the phosphorus that carry the Ph groups and positive on the phosphorus that carry the ^{i}Pr groups.

4.6 Conclusion

Pulsed EPR/ENDOR experiments at 95 GHz have been shown feasible for a bidentate high-spin ($S = 3/2$) Co^{2+} complex in which the cobalt is coordinated by four sulfur atoms. From the study of the ESE-detected EPR spectra of a diamagnetically diluted 1% $Co^{iPr,Ph}L_2/Zn^{iPr,Ph}L_2$ crystal as a function of the orientation of the magnetic field with respect to the crystal, the orientation of the principal axes of the effective g' tensor could be determined. This in turn enabled the study of the pulsed ENDOR spectra as a function of the orientation of the magnetic field in this molecule-fixed axes system.

The ENDOR spectra revealed signals from ligand phosphorus nuclei, which were analyzed in detail and complete hyperfine tensors were obtained for all four phosphorus atoms in the complex. On the basis of the anisotropic parts, the tensors could be assigned to the two types of phosphorus present, the phosphorus that carry two Ph groups and the phosphorus that carry two ^{i}Pr groups. The isotropic hyperfine interactions of the differently substituted phosphorus have opposite sign. The phosphorus hyperfine tensors reveal the asymmetry in the delocalization of the spin density from cobalt over the ligand. This implies that the Co−S bonds are non-equivalent as a result of a subtle difference far away from the $Co(II)S_4$ core.

4. A W-band pulsed EPR/ENDOR study of Co(II)S_4 coordination in the Co[$(SPPh_2)(SP^iPr_2)N]_2$ complex